Vietnam Journal of Catalysis and Adsorption
Tạp chí xúc tác và hấp phụ Việt Nam

https://jca.edu.vn

Sulfur-Doped Graphitic Carbon Nitride for Photocatalytic degradation of Congo Red Removal: Synthesis and Performance Analysis

Nguyen Ngoc Tue[1], Pham Van Anh[1], Le Thi Diem Quynh[1], Nguyen Xuan Truong[1], Nguyen Duc Trung[1,*]

[1] *Department of Chemistry, School of Chemistry and Life Sciences , Hanoi University of Science and Technology, Hanoi, Vietnam*
** Email: trung.nguyenduc1@hust.edu.vn*

ARTICLE INFO

Received: 08/12/2024
Accepted: 30/03/2025
Published: 30/03/2025

Keywords:
Graphitic carbon nitride; g-C3N4; Design strategies; Photocatalysis; Reaction mechanism

ABSTRACT

This study explores the effective synthesis of sulfur-doped graphitic carbon nitride (S-doped g-C_3N_4) and its application in the photocatalytic degradation of the organic dye Congo Red (CR). By systematically varying the ratios of thiourea and urea during synthesis, the structural and photocatalytic properties of the resulting materials were optimized. Characterization via X-ray diffraction (XRD) and Fourier-transform infrared spectroscopy (FT-IR) confirmed that the S-doped g-C_3N_4 samples retained the characteristic crystal structure of pristine g-C_3N_4 while successfully incorporating sulfur atoms into the lattice. The iSCN1 sample exhibited superior photocatalytic performance, achieving a CR removal efficiency of 93.2% within 90 minutes in a 10 mg/L solution, outperforming undoped g-C_3N_4. Moreover, the addition of hydrogen peroxide H_2O_2 significantly enhanced the degradation rate, allowing iSCN1 to achieve 91.8% CR removal within just 60 minutes under comparable radiation exposure. Resutls from the radical trapping experiment revealed that hydroxyl radicals (•OH) generated during the photocatalytic process played a critical role in the CR decomposition reaction. The improvement in photodegradation efficiency results from the delocalization of lone electrons, which facilitates the separation of photogenerated charges, alongside the increased band gap of S-doped g-C_3N_4. These findings demonstrate the potential of S-doped g-C_3N_4 as an advanced photocatalyst for wastewater treatment applications and provide valuable insights into optimizing its synthesis for enhanced environmental remediation efficiency.

Introduction

In the 21st century, the foremost developing challenges are the global energy problem and environmental pollution. Environmental pollution, particularly water contamination with organic dyes, poses a significant threat to ecosystems and human health. These urgent concerns are propelled by the swift expansion of population and industrialization [1, 2]. The global reliance on finite energy resources and the escalating pressure from these challenges have rendered the quest for the discovery, utilization, and storage of renewable energy critical, garnering worldwide scientific attention. Photocatalysis, a substance that harnesses readily accessible solar energy, has emerged as a significant research focus in addressing the energy crisis. Despite

https://doi.org/10.62239/jca.2025.013

the abundance and continuity of solar energy, only fifty percent of sunlight's energy can be harnessed upon reaching the Earth's surface. The effective utilization of this light source remains a considerable issue. Consequently, it is essential to investigate appropriate photocatalysts that optimize photocatalytic reactions while ensuring their stability [3,4]. Research has been conducted on CdS, TiO_2, ZnO, among others; however, these photocatalytic materials exhibit very low solar energy usage efficiency and quantum yield [5,6]. Carbon nitride, a graphene-like semiconductor material (g-C_3N_4), comprises triazine interconnected with tertiary ammonia. This semiconductor material possesses a bandgap value of 2.7 eV, absorbs light within the visible spectrum, and exhibits both thermodynamic and chemical stability. A 2009 study shown that g-C_3N_4 can engage in the hydrogen evolution reaction utilizing 10 vol.% triethanolamine (TEOA) under visible light exposure. g-C_3N_4 can activate oxygen and directly or indirectly facilitate the production of free radicals involved in the redox process, owing to interlayer bonding via van der Waals forces and the substantial reduction potential of the valence band. In 2023, Zuo *et al.* found that sulfur-doped carbon nitride efficiently addressed the shortcomings of conventional anion doping, which frequently diminishes redox potential and carrier mobility [7]. Altering the electrical structure of semiconductor photocatalysts enables them to attain a broader absorption spectrum. This advancement introduces a novel method for synthesizing high-performance photocatalysts by elemental doping. Consequently, numerous research have examined the integration of sulfur monomers into carbon nitride. In 2012, Chen *et. al.* utilized density functional theory to develop the layered interlayer architecture of sulfur-doped carbon nitride. It was discovered that sulfur atoms substituted nitrogen atoms in instances where two contiguous carbon atoms were linked. Sulfur doping of carbon nitride produced a significant red shift in its light absorption spectrum, signifying improved photocatalytic effectiveness of sulfur-doped carbon nitride [8.]

The incorporation of sulfur into g-C_3N_4 nanosheets significantly increases the specific surface area, boosts light absorption, and enhances the separation efficiency of photo-induced charge carriers, leading to a remarkable improvement in photocatalytic activity. To comprehend the underlying mechanism, multiple characterizations have been performed on the synthesized photocatalysts. This project involved the synthesis of S-doped g-C_3N_4 materials for the removal of the organic dye Congo Red.

Experimental

Chemicals

Urea $(NH_2)_2CO$, Thiourea $(NH_2)_2CS$ and Crystal Violet were purchased from Xilong Inc., Ltd. (China). All the chemicals were of reagent grade (99% purity) and used without further purification.

Material synthesis

For the synthesis of the undoped g-C_3N_4, ten grams of 99% urea solid powder were calcined in a crucible at 500°C, maintained at this temperature for two hours under air pressure, with a heating rate of 2°C/min. The acquired light yellow solid was examined for features including crystal structure and characteristic chemical bonding of the material. For the synthesis of the S doped g-C_3N_4, a quantity of 10 grams of 99% urea were dissolved in a beaker containing 10 milliliters of water and agitated for 30 minutes, resulting in solution A. An adequate quantity of thiourea at ratios of 0.1%, 0.5%, 1.0%, and 2.0% relative to the urea content was incorporated into the aforementioned solution. Once the thiourea was fully dissolved, the system's temperature was elevated to around 80-85^{0}C. Agitate the aforementioned solution until full crystallization occurs. The solid was calcined by heating from ambient temperature to 550°C and sustaining this temperature for 2.5 hours at a rate of 1°C/min. The samples are labeled based on impurity concentration as iSCNx, where x = {1,2,3,4} corresponds to precursor percentages of 0.1%, 0.5%, 1.0%, and 2.0%, respectively.

Structural analysis

The attributes of the crystal lattice composition and structure of g-C3N4 and its doped variants were determined using X-ray diffraction (XRD) employing Cu-Kα radiation. Infrared spectroscopy was employed to ascertain the functional groups present on the material surface. XRD and FT-IR analyses of the material samples were performed at Hanoi University of Science and Technology. The concentration of Congo Red (CR) in the experiments was measured using a UV-Vis spectrophotometer (DR-3900) at the Department of Chemistry, School of Chemistry and Life Sciences, HUST. CR standard solutions were meticulously constructed to establish a standard curve for quantifying CR content. This involved examining the material's capacity to remediate Congo Red (CR) dye. A series of material with the mass varying between 0.03 and 0.05 g were transfered into a conical flask, subsequently adding 100

https://doi.org/10.62239/jca.2025.013

mL of a 10 mg/L CR solution. The reaction system was first performed in darkness, kept stirring for 30 minutes, and subsequently exposed to a 250 W incandescent bulb for 80 to 150 minutes. The system's temperature was maintained at a consistent level by a thermostat, specifically at room temperature, 25 degree of Celcisus. After 10-minute intervals, roughly 3-5 ml of the suspension was extracted from the device, utilizing a syringe to filter the suspension and get a clear solution. The optical density was subsequently measured using a UV-VIS equipment at specified time intervals. The identical approach was reiterated in trapping experiment to ascertain the free radicals produced by the addition of 2-propanol (IPA).

Kinetics experiment

Each experiment has been repeated four times to make sure the repeatability and reliability. Concentrations of the dyes were estimated using the linear regression equations (obtained by plotting its calibration curve). The amount of adsorbed the two dyes by adsorbent (q_e (mg/g)) was calculated by the following equation

$$q_e = \frac{(C_0 - C_e)V}{W}$$

where C_0 and C_e are the initial and equilibrium concentrations of the adsorbates (in this case CR), respectively. V represents the volume of the solution in liters, in this case, V = 0.1 L and M is the mass of the adsorbent in grams. The experiments were conducted with and without radiation to evaluate the CR remocal efficiency.

Results and discussion

XRD study

Initially, the crystal features of the g-C_3N_4 and the S-doped g-C_3N_4were studied to establish structure-property relationships. The crsytal characteristics of materials observed in X-ray Diffraction (XRD) are shown in Fig 1. The XRD spectrum of pure g-C_3N_4 and S-doped g-C_3N_4 samples (iSGN1, iSGN2, iSGN3, and iSGN4) offers significant insights into the structural alterations caused by sulfur doping. In pristine g-C_3N_4, the distinctive diffraction peaks at 27.4° and 13.1° correspond to the (002) and (100) planes, respectively, indicating the interlayer stacking of aromatic systems and the in-plane structural arrangement of g-C_3N_4. These peaks validate the characteristic graphitic structure. Significant alterations are evident in the XRD patterns following sulfur doping. The (002) peak of the S-doped samples shifts somewhat toward lower angles, signifying an augmented interlayer space resulting from the introduction of sulfur atoms, which possess a bigger atomic radius than the nitrogen or carbon atoms they supplant. The enlargement of the lattice structure indicates effective doping. Furthermore, the (002) peak broadens with elevated sulfur content, indicating a decrease in crystallinity due to structural distortions resulting from doping.

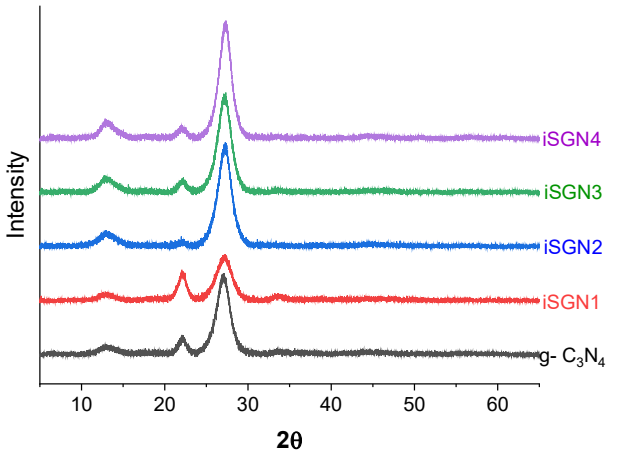

Fig. 1. The XRD spectra of the undoped g-C_3N_4 and the four S-doped g-C_3N_4 with varied S component

The peak intensities diminish progressively from iSGN1 to iSGN4, indicating that increased sulfur concentration impairs the long-range order of the graphitic layers. A detailed examination of the S-doped samples indicates that iSGN1 (0.1% sulfur) maintains a structure most akin to that of pure g-C_3N_4, exhibiting minor peak shifts or broadening, which suggests a relatively low degree of structural perturbation. Conversely, iSGN2 (0.5%) and iSGN3 (1%) demonstrate more pronounced shifts, broadening, and intensity diminutions, indicative of moderate doping levels that induce considerable lattice modifications. iSGN4 (2%), the sample exhibiting the greatest sulfur concentration, demonstrates the most significant structural alterations, characterized by peak broadening and diminished intensity, underscoring the considerable structural disorder induced by over-doping. The structural modifications significantly affect the photocatalytic efficacy of the materials. The augmented interlayer spacing and diminished crystallinity in the S-doped samples promote photocatalytic activity by promoting charge separation, optimizing charge transport, and augmenting the accessibility of surface-active sites. Excessive sulfur doping, as observed in iSGN4, may undermine the material's structural integrity and performance due to significant lattice distortions. Moderate doping levels, as seen in iSGN1 and iSGN2, maintain structural integrity while producing advantageous flaws, resulting in improved photocatalytic performance. The XRD data

validate that sulfur doping significantly alters the structural characteristics of g-C_3N_4, corresponding with the noted enhancements in the photocatalytic degradation efficiency of Congo Red.

Fig. 2 illustrates the FT-IR spectra of pure g-C_3N_4 (at the bottom) and S-doped g-C_3N_4 samples (iSGN1, iSGN2, iSGN3, and iSGN4) underscore the structural modifications induced by sulfur doping. In the undoped g-C_3N_4, the distinctive absorption bands are observed between 1200 and 1700 cm^{-1}, corresponding to the stretching vibrations of C=N and C-N bonds inside the heptazine units that constitute the graphitic structure. The notable peak at 807 cm^{-1} is ascribed to the out-of-plane bending vibration of triazine rings, a characteristic property of g-C_3N_4. The extensive absorption band at 3182 cm^{-1} corresponds to the stretching vibration of N-H bonds, indicating the existence of uncondensed amino groups or structural flaws at the margins. The S-doped samples retain their overall spectrum characteristics, demonstrating that the heptazine-based framework of g-C_3N_4 is unaltered during the doping process. Notable alterations are evident in the strength and morphology of the peaks, indicating the integration of sulfur atoms into the lattice. The bands in the 1200–1400 cm^{-1} range, linked to C-N stretching vibrations, exhibit a small broadening and reduction in intensity with elevated sulfur content, likely due to structural deformation and the replacement of nitrogen by sulfur in the graphitic network. The peak at 1079 cm−1, presumably resulting from C-S stretching vibrations, is present in the doped samples, thereby affirming the successful integration of sulfur atoms. The peak is more prominent in iSGN3 and iSGN4, signifying elevated sulfur doping levels. Additionally, the N-H stretching band at 3182 cm^{-1} exhibits a modest shift and broadening in the doped samples, maybe due to interactions between sulfur atoms and amino groups, which modify the hydrogen bonding environment. The triazine bending vibration at 807 cm^{-1} exhibits negligible positional alterations, although its intensity diminishes with increasing doping levels (iSGN3 and iSGN4), indicating a decline in the long-range ordering of the triazine units attributable to doping-induced structural flaws. In comparison, the doped samples iSGN1 and iSGN2, which have little sulfur concentration, demonstrate highly preserved spectral characteristics, signifying no disturbance to the framework. Conversely, iSGN3 and iSGN4, which possess elevated sulfur content, exhibit more significant alterations, including the broadening and attenuation of critical peaks, indicative of heightened disorder and structural modification. The findings indicate that sulfur doping adds new functional groups (e.g., C-S) and alters the bonding environment, which is anticipated to affect the electrical structure and photocatalytic activities. The FT-IR research conclusively demonstrates effective sulfur doping and elucidates the influence of sulfur content on the structural and vibrational characteristics of g-C_3N_4.

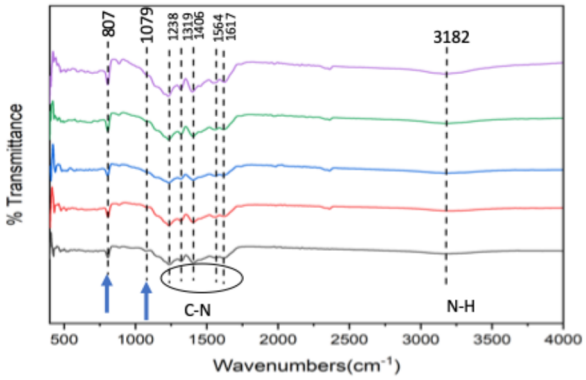

Fig. 2. The FT-IR spectra of the undoped g-C_3N_4 and the four S-doped g-C_3N_4 with varied S component

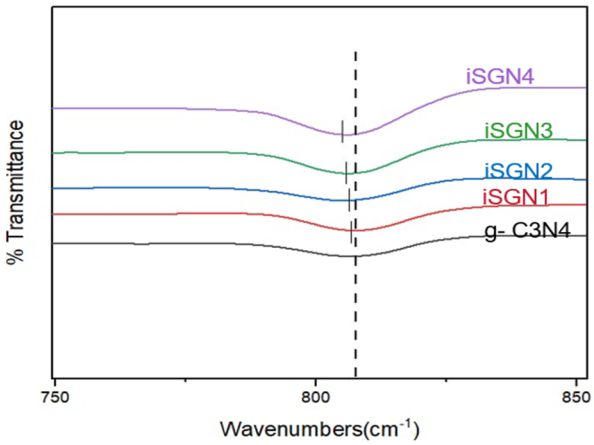

Fig. 3. The FT-IR spectra at 807 cm^{-1} range of the undoped g-C_3N_4 and the four S-doped g-C_3N_4 with varied S component

The adsorption investigation in Fig. 4 of undoped g-C_3N_4 and sulfur-doped g-C_3N_4 (iSGN1, iSGN2, iSGN3, and iSGN4) demonstrates notable enhancements in the adsorption characteristics of the doped materials, principally due to structural modifications resulting from sulfur inclusion. The experimental data indicate that all materials attain quick adsorption equilibrium after approximately 30 minutes in the absence of light, after which the adsorption capacity stays predominantly stable. This swift equilibrium indicates a strong interaction affinity between the materials and the dye molecules. The pure g-C_3N_4 demonstrates a comparatively lower adsorption capacity of roughly 15 mg/g, which markedly rises with sulfur doping, to a

https://doi.org/10.62239/jca.2025.013

maximum of about 25 mg/g for iSGN1 and iSGN2. The results indicate that sulfur doping significantly improves the adsorption capability of the g-C_3N_4 material. The trend of enhanced adsorption capacity with elevated sulfur concentration underscores the pivotal function of sulfur atoms in altering the material's characteristics. The enhanced adsorption efficacy of the doped materials is ascribed to the alterations in the crystal lattice structure caused by sulfur doping. The introduction of sulfur atoms into the semiconductor lattice creates structural flaws and modifies the electronic environment, hence enhancing the quantity of active adsorption sites. Furthermore, sulfur doping may augment the material's surface polarity, hence enhancing its interaction with polar dye molecules such as Congo Red. The minor variations in adsorption capacity among the samples (iSGN1, iSGN2, iSGN3, and iSGN4) indicate that excessive sulfur doping, particularly in iSGN4, may result in the saturation of active sites or aggregation, hence marginally diminishing adsorption efficiency relative to optimal doping levels. The sulfur-doped g-C_3N_4 materials exhibit enhanced adsorption capacity owing to the augmented number of active sites and improved interaction potential, rendering them highly efficient for dye removal via the adsorption mechanism. These findings highlight the significance of sulfur doping as a method to enhance the efficacy of g-C_3N_4 for environmental remediation purposes.

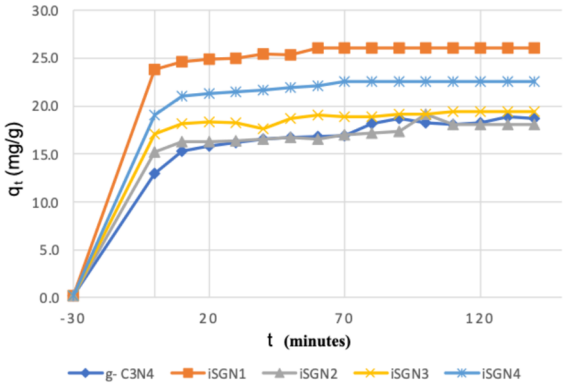

Fig. 4. The adsorption of undoped g-C_3N_4 and the four S-doped g-C_3N_4. The experiments were all conducted in the dark conditions

The photocatalytic properties of four S-doped g-C_3N_4 are strongly evidenced by the significant enhancement in Congo Red (CR) removal efficiency under visible light compared to dark conditions. For pristine g-C_3N_4, the dye treatment efficiency increased from 56% in the dark to 90% under visible light after 150 minutes, confirming its inherent photocatalytic activity. This improvement, an increase of approximately 34%, underscores the role of light in activating the material to produce reactive species for dye degradation. The sulfur-doped variants further amplify this photocatalytic effect, as evidenced by the experimental results comparing the treatment efficiencies under visible light for the doped samples. Among the S-doped materials, iSGN1 exhibited the highest dye removal efficiency, achieving 93.2% in just 90 minutes, significantly outperforming pristine g-C_3N_4 This accelerated and improved photocatalytic performance is attributed to sulfur doping, which enhances the material's electronic structure by introducing mid-gap states and increasing the separation and mobility of photogenerated charge carriers. The enhanced performance of iSGN1 can be explained by the optimal sulfur content, which effectively introduces structural defects and active sites without excessively disrupting the crystal lattice. These structural changes lead to higher photon absorption, better charge carrier dynamics, and an increased generation of reactive species, such as hydroxyl radicals (•OH), which are critical for CR degradation. The shorter time required for iSGN1 to reach the highest treatment efficiency compared to other doped samples and pristine g-C_3N_4 further highlights its superior photocatalytic performance. In contrast, over-doping, as observed in samples with higher sulfur content like iSGN4, may result in a slight decrease in performance due to excessive structural distortion and recombination of charge carriers. Collectively, these results clearly demonstrate that sulfur doping not only improves the photocatalytic efficiency of g-C_3N_4 under visible light but also optimizes the reaction kinetics, making S-doped g-C_3N_4 a promising candidate for photocatalytic degradation of organic dyes like CR in wastewater treatment. The effiecy of removing CR by five material and comparing with the materials synthesized by Kumar and his coworker [10].

Table 1. The effciciency of removing CR by five materials

Materials	t (Minutes)	Efficiency (%)	
		Light	Dark
g- C_3N_4	150	88.7	56.8
iSGN1	90	93.2	78.4
iSGN2	110	83.9	54.2
iSGN3	120	91.3	58.4
iSGN4	80	90.7	67.7
KGM[10]	60	76	

The removal efficiency of CR dye is significantly influenced by both the mass of the catalyst and the concentration of H_2O_2, as evidenced by systematic

experiments. When varying the mass of the iSGN1 material in a 10 mg/L CR solution under visible light, an increase in the catalyst mass consistently resulted in enhanced dye treatment efficiency and faster degradation rates. This relationship highlights the critical role of active surface area and available active sites in accelerating the photocatalytic process. However, beyond 30 mg of catalyst, the improvement in efficiency plateaued, suggesting a threshold where excess material leads to aggregation or light scattering effects that diminish the accessibility of light energy and active sites. This observation underscores the importance of optimizing the material mass for efficient photocatalytic reactions. The addition of H_2O_2 further amplified the photocatalytic performance of the iSGN1 material by acting as an external source of hydroxyl radicals (•OH), which are pivotal in the oxidative degradation of organic dyes. When H_2O_2 was introduced after the system reached equilibrium in the dark, the treatment efficiency improved significantly across all material samples, and the reaction time to achieve high degradation rates was shortened. This demonstrates the synergistic role of H_2O_2 in enhancing the density of reactive species in the solution, thereby facilitating more rapid CR decomposition. The concentration of H_2O_2 , however, played a nuanced role in the process. At 5 mM, the treatment efficiency reached 91.8%, the highest among the tested concentrations. In contrast, higher concentrations such as 10 mM (81.2%) and 15 mM (88.6%) resulted in slightly reduced efficiencies, likely due to the self-scavenging effect of excess H_2O_2, which consumes hydroxyl radicals, reducing their availability for dye degradation.

Also, in the trapping experiement, it clearly showed that the OH play an crtical role in removing the CR. The graph illustrates the effect of isopropanol (IPA), a hydroxyl radical (•OH) scavenger, on the photocatalytic degradation of Congo Red (CR) over time. As the concentration of IPA increases from 0 mM to 1.00 mM, the degradation efficiency decreases significantly, confirming the critical role of •OH radicals in the photocatalytic process. Without IPA (0.00 mM), the CR degradation is most effective, indicating a high generation of reactive •OH species. At 0.25 mM IPA, the degradation rate is slightly reduced, while at 0.50 mM and 1.00 mM IPA, the inhibition of CR removal becomes more pronounced, as IPA competes with CR molecules for •OH radicals. This trend strongly suggests that •OH radicals are primary active species driving the decomposition of CR in the photocatalytic system. The results highlight the essential role of •OH radicals in enhancing photocatalytic performance and confirm their involvement in the degradation mechanism.

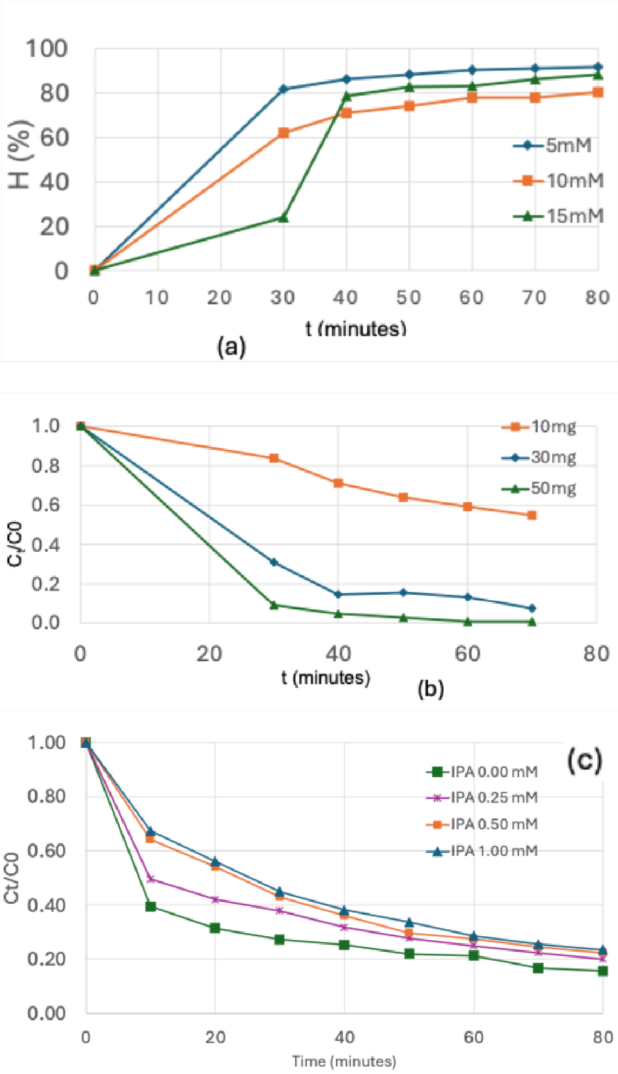

Fig 2. (a) The effect of the concentration of H_2O_2 upon the removal efficiency, (b) the effect of mass of sample upon the removal and (c) the trapping experiment in which the IPA concentration varied from 0.00 to 1.00 mM

These results highlight the effectiveness of the iSGN1 material as a heterogeneous photocatalyst and underscore the importance of optimizing both the catalyst mass and the H_2O_2 concentration for achieving maximum dye treatment efficiency. The combination of sulfur doping and H_2O_2 addition not only retains the structural integrity of the material but also significantly enhances its photocatalytic properties, making iSGN1 the most efficient among the tested samples under optimized conditions. These findings provide valuable insights into designing effective photocatalytic systems for environmental remediation.

https://doi.org/10.62239/jca.2025.013

Conclusion

This study successfully demonstrated the synthesis and application of S-doped g-C_3N_4 as an efficient photocatalyst for the removal of Congo Red dye. The optimized sample, iSCN1, showed enhanced photocatalytic performance, attributed to the increased surface area and the presence of reactive hydroxyl radicals. The findings provide valuable insights into the design and fabrication of novel heterogeneous photocatalysts, offering a promising strategy for addressing environmental pollution.

Acknowledgments

This research is funded by the Science and Technology Tasks under the Protocol with Hungary under project number NĐT/HU/22/21.

References

1. M. Ismael, J Alloys Compd 931 (2023) 167469. https://doi.org/10.1016/j.jallcom.2022.167469

2. R. Singh, M. Chauhan, P. Garg, B. Sharma, P. Attri, R.K. Sharma, D. Sharma, G.R. Chaudhary, J Clean Prod 427 (2023). https://doi.org/10.1016/j.jclepro.2023.138855

3. D. Gang, Z. Uddin Ahmad, Q. Lian, L. Yao, M.E. Zappi, Chemical Engineering Journal 403 (2021) 126286. https://doi.org/10.1016/j.cej.2020.126286

4. G.Q. Zhao, J. Zou, J. Hu, X. Long, F.P. Jiao, Sep Purif Technol 279 (2021). https://doi.org/10.1016/j.seppur.2021.119769.

5. D. Beydoun, R. Amal, G.K.C. Low, S. McEvoy, Journal of Physical Chemistry B 104 (2000) 4387–4396. https://doi.org/10.1021/jp992088c

6. A. Petrosyan, L. Zach, T. Taeufer, T.S. Mayer, J. Rabeah, J. Pospech, Chemistry - A European Journal 28 (2022). https://doi.org/10.1002/chem.202201761

7. K. Maeda, X. Wang, Y. Nishihara, D. Lu, M. Antonietti, K. Domen, The Journal of Physical Chemistry C 113 (2009) 4940–4947. https://doi.org/10.1021/jp809119m

8. M. Zuo, X. Li, Y. Liang, F. Zhao, H. Sun, C. Liu, X. Gong, P. Qin, H. Wang, Z. Wu, L. Luo, Sep Purif Technol 308 (2023). https://doi.org/10.1016/j.seppur.2022.122875

9. G. Chen, S.-P. Gao, Chinese Physics B 21 (2012) 107101. https://doi.org/10.1088/1674-1056/21/10/107101

10. R. Kumar, A.A.P. Khan, A. Sudhaik, S. Sonu, S. Kaya, P. Singh, P. Raizada, M.E.M. Zayed, M.N. Arshad, K.A. Alzahrani, Nano Express 6 (2025) 015009. https://doi.org/10.1088/2632-959X/ad93eb